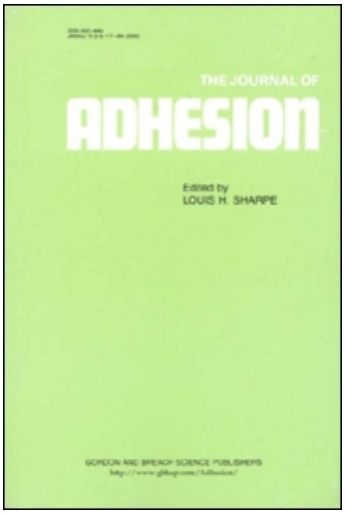

The Journal of Adhesion
Publication details, including instructions for authors and subscription information:
http://www.informaworld.com/smpp/title~content=t713453635

Application of Caustic Foci to Measure Small Dimensional Changes Accompanying Water Uptake by Polymer Coatings on the Chip-on-board (COB)

Z. R. Xu[a]; K. H. G. Ashbee[a]
[a] Center for Materials Processing and Dept. of Materials Science and Engineering, The University of Tennessee, Knoxville, TN, U.S.A.

To cite this Article Xu, Z. R. and Ashbee, K. H. G.(1991) 'Application of Caustic Foci to Measure Small Dimensional Changes Accompanying Water Uptake by Polymer Coatings on the Chip-on-board (COB)', The Journal of Adhesion, 35: 2, 135 — 161
To link to this Article: DOI: 10.1080/00218469108030442
URL: http://dx.doi.org/10.1080/00218469108030442

J. Adhesion, 1991, Vol. 35, pp. 135–161
Reprints available directly from the publisher
Photocopying permitted by license only

Printed in the United Kingdom

Application of Caustic Foci to Measure Small Dimensional Changes Accompanying Water Uptake by Polymer Coatings on the Chip-on-board (COB)

Z. R. XU and K. H. G. ASHBEE*

Center for Materials Processing and Dept. of Materials Science and Engineering, The University of Tennessee, Knoxville, Knoxville, TN 37996–2200, U.S.A.

(Received January 28, 1991; in final form April 28, 1991)

As deposited, the protective silicone coating applied to electronic packages, such as the chip-on-board (COB), has smoothly curved edges that can be sufficiently reflective to generate optical caustic foci. The geometry of caustic foci is extremely sensitive to the topography of the reflecting surface. We have exploited this fact to develop a new method for monitoring surface distortion during swelling (or shrinkage) associated with the presence of diffused water within the material of the sealant.

KEY WORDS caustic foci; measurement of small deformation; water uptake; polymer coating; electronic package.

INTRODUCTION

Caustics are the most general way of describing the focusing of a wavefield. They are surfaces of high wave intensity as opposed to the point focus of paraxial optics. The defect known as spherical aberration arises for nonparaxial rays from the dependence of focal length on aperture size; marginal rays undergo more refraction than do paraxial rays and are focused in front of the paraxial rays. The resulting envelope of the refracted rays, illustrated in Figure 1, is called a caustic.[1] Generally speaking, caustics are curves to which the light rays are tangential, and on one side of which the intensity of light is enhanced and on the other side it is zero. One of the easiest caustics to observe is that which forms in a cup of coffee.

Ray diagrams are formulated such that the intensity of radiation is proportional to the density of rays. Hence, it is evident that the energy is highly concentrated in the vicinity of the caustic. In fact, it can be shown that the density of rays is infinite thereabout, implying that a more accurate model of the wavefield is required in the

*Corresponding author. Present address: 32, Heathgate, Yatton, Bristol BS19 4DY, UK

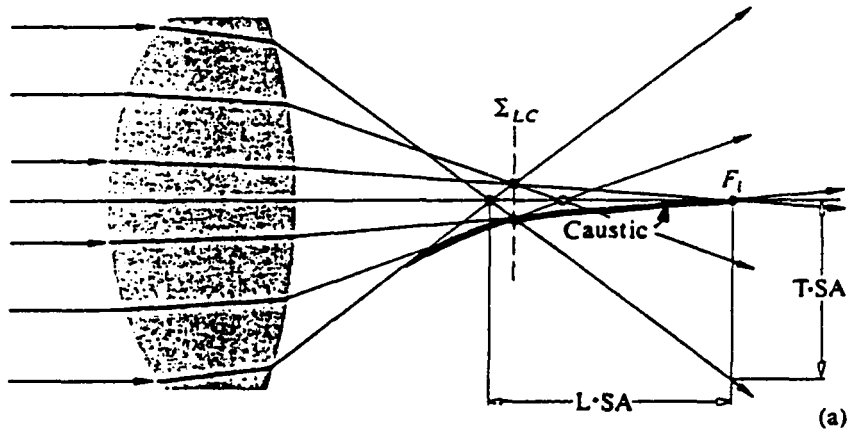

FIGURE 1 Spherical aberration for a lens. The envelope of the refracted rays is called a caustic. (Source: Hecht[1]).

region of such a singularity. It can also be seen from Figure 1, that the caustic forms a well-defined boundary within a set of rays; on crossing a caustic, one moves from a region of shadow into one of illumination.

Consider the simple case shown in Figure 2, where a parallel beam of light along the Z-axis is incident on a curved surface S

$$Z = S(x,y) \tag{1}$$

The light reflected from the surface obeys the well-known laws of reflection. An incident ray and its reflected ray are shown in Figure 2. The reflected rays are intercepted by the screen at a point (u,v). Using Snell's law, the correspondence between points on the same ray of light in the surface, S(x,y), and on the screen is given by

$$\begin{aligned} u &= x + [z_o - S(x,y)] \tan 2\alpha \\ v &= y + [z_o - S(x,y)] \tan 2\beta \end{aligned} \tag{2}$$

where x, y are co-ordinates in the surface S(x,y) and u, v are co-ordinates on the screen. α and β, the angles of incidence on S(x,y) for a given ray, measured in the xoz- and yoz-planes, respectively, are given by

$$\begin{aligned} \tan\alpha &= \frac{\partial S(x,y)}{\partial x} \\ \tan\beta &= \frac{\partial S(x,y)}{\partial y} \end{aligned} \tag{3}$$

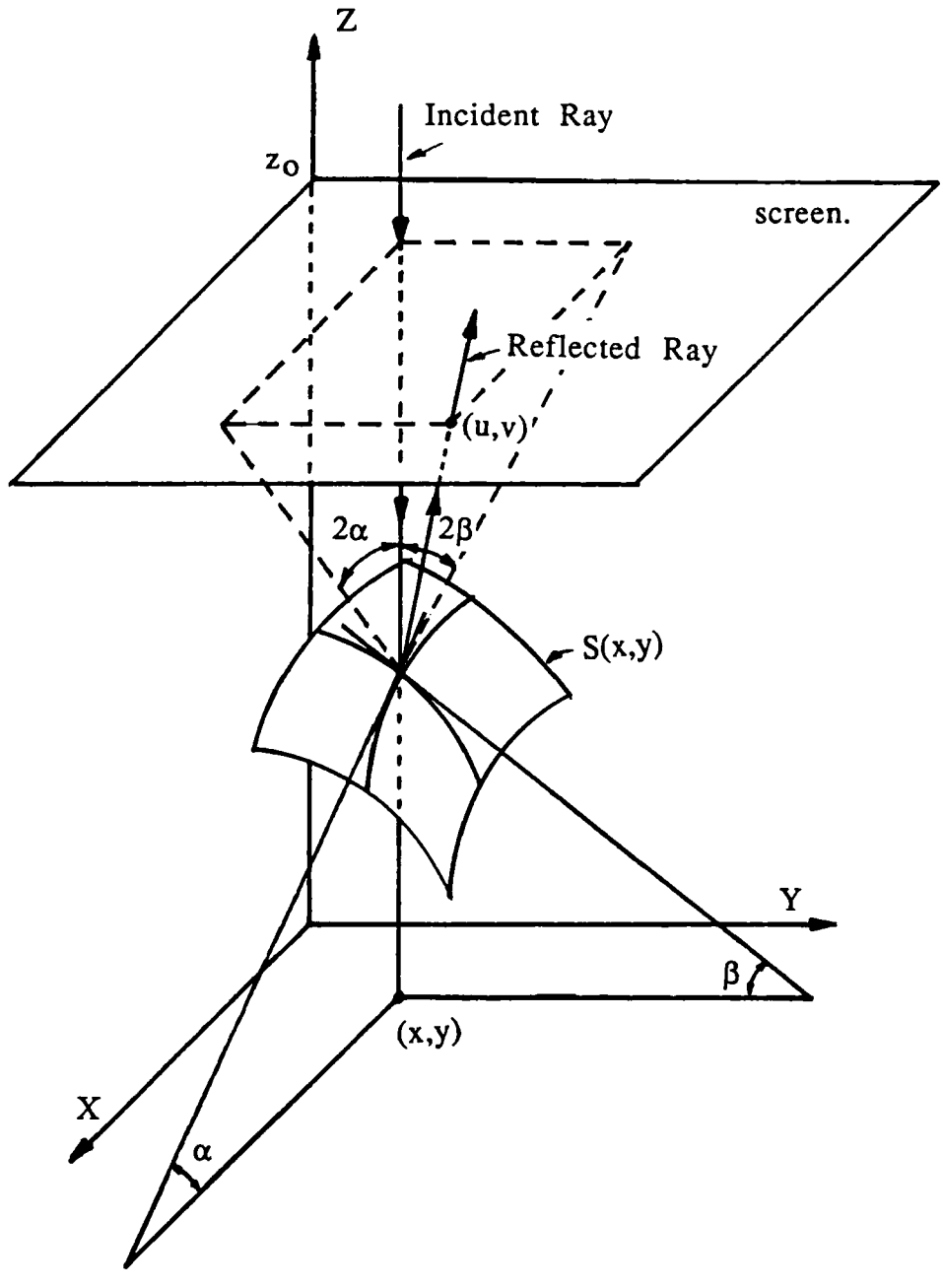

FIGURE 2 Geometrical relationship between incident ray and reflected ray in 3 dimensions.

Substituting Eq. (3) into Eq. (2), the image on the screen of any point of the surface is given by

$$u = x + [z_o - S(x,y)] \frac{2\frac{\partial S(x,y)}{\partial x}}{1 - \left[\frac{\partial S(x,y)}{\partial x}\right]^2}$$
$$v = y + [z_o - S(x,y)] \frac{2\frac{\partial S(x,y)}{\partial y}}{1 - \left[\frac{\partial S(x,y)}{\partial y}\right]^2} \tag{4}$$

Eq. (4) is the optical transform that relates the reference surface S(u,v) to the specimen surface S(x,y). In order for a caustic to form on the surface (u,v) as the reflecting point x,y moves around on the surface S, we must generate a boundary curve on u, v between a region where reflected rays are concentrated and a region from which they are absent. Where this curve is parallel to the u-axis, v must take a maximum or minimum value and, conversely, for segments parallel to the v-axis, u must take a maximum or minimum value. These are, in fact, the general conditions necessary for a caustic and can be expressed mathematically as follows,

$$J = \frac{\partial(u,v)}{\partial(x,y)} = \begin{bmatrix} \frac{\partial u}{\partial x} & \frac{\partial u}{\partial y} \\ \frac{\partial v}{\partial x} & \frac{\partial v}{\partial y} \end{bmatrix} = 0 \tag{5}$$

The use of caustics as an experimental probe is relatively new. It was originally introduced by Manogg[2] for investigating crack tip stress intensifications. The method is sensitive to gradients of elastic displacement and is, therefore, an appropriate tool for investigating stress concentration problems. The technique was later extended for the same purpose by Theocaris,[3] and by Kalthoff[4] to explore material behavior under various static and dynamic loading conditions. Recently, Brewster[5] has further developed the technique for ultrasonic non-destructive evaluation purposes.

A NEW METHOD TO MEASURE SMALL DEFORMATION

That the phenomenon known as an optical caustic is related to the geometric optics of light rays reflected by a curved surface has been introduced. The physical principles and the mathematical description of caustics will now be presented in order to develop a new method to measure small changes in curvature of such a surface.

In Figure 3, consider the goemetry of a caustic associated with a surface, initially

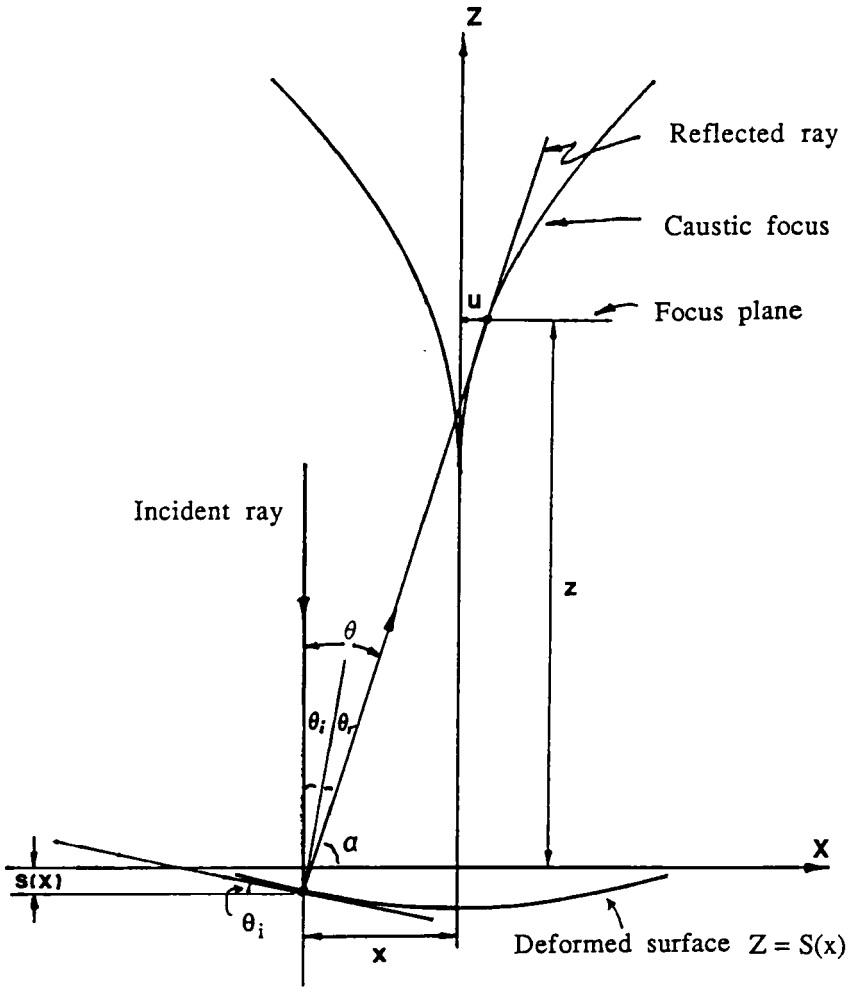

FIGURE 3 The caustic geometry associated with a surface deformed from flat to cylindrical shape.

flat, that has been deformed to a surface of cylindrical symmetry, for the sake of simplification. The angle of incidence equals the angle of reflection, that is,

$$\theta_i = \theta_r \tag{6}$$

Since

$$\theta_i = \tan^{-1}\left(\frac{ds}{dx}\right) \tag{7}$$

$$\alpha = 90° - 2\tan^{-1}\left(\frac{ds}{dx}\right) \tag{8}$$

Thus the orientation of the reflected ray is such that the geometry of the caustic is a function of a gradient of the displacement field, $\frac{ds}{dx}$.

Consider a parallel beam of light incident along the Z-axis in Figure 3. Let it illuminate a curved surface, S, of cylindrical symmetry,

$$Z = S(x) \tag{9}$$

Referring to Figure 3, correspondence between points in the surface, S, and in the focus plane, S_f, for a given light ray, is expressed by,

$$u - x = [z - S(x)] \tan\theta \tag{10}$$

where, for a given ray, x is its co-ordinate in the surface S and u is its co-ordinate in the focus plane S_f.

Using the condition for formation of caustic foci, in Eq. (5), we can obtain

$$z = S + \left(\tan\theta \frac{dS}{dx} - 1\right) \cos^2\theta \frac{dx}{d\theta} \tag{11}$$

$\frac{dx}{d\theta}$ can be derived and is given by

$$\frac{dx}{d\theta} = \frac{1 + S_x^2}{2S_{xx}} \tag{12}$$

where $S_x = \frac{dS}{dx}$, $S_{xx} = \frac{d^2S}{dx^2}$.

Substituting Eq. (11) into Eq. (10),

$$u = x + \left(\tan\theta \frac{dS}{dx} - 1\right) \cos^2\theta \tan\theta \frac{dx}{d\theta} \tag{13}$$

Eqs. (11) and (13) are the required relationships between the deformation, S and $\left(\frac{dS}{dx}\right)$, of the reflecting surface and the co-ordinate, (u,v), of the caustic focus. Measurement of the latter can evidently be used to determine the deformation of the reflecting surface.

If Figure 3 represents a surface of small slope,

$$\tan\theta_i \approx \theta_i$$

The relationship between the deformation of the reflecting surface and the co-ordinate of the caustic focus becomes

$$z = \frac{1}{2S_{xx}}$$

$$u = x - \frac{S_x}{S_{xx}} \tag{14}$$

Note that,

$$\frac{d^3S}{dx^3} = 0 \text{ at the cusp point in a caustic focus.}$$

In this case, values for $\frac{d^2S}{dx^2}$, the second differential of the surface displacement, can be obtained directly from the caustic focus. Referring to Figure 4, the turning points A, B and B′ can be located by inspection of the geometry of the caustic focus and, by sketching in the intermediate points, the overall shape of the second differential of the reflecting surface can be deduced immediately. Note that the second differential of the displacement field of a thin plate is a measure of the bending moment. Furthermore, by differentiating two more times to get the 4th

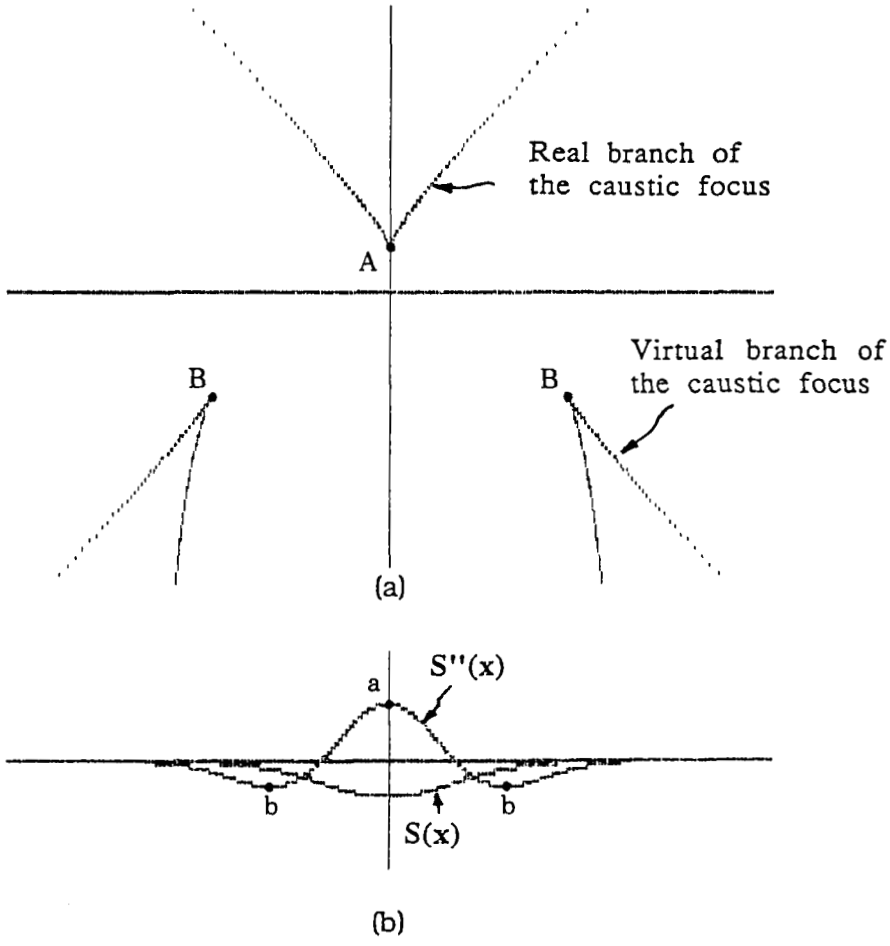

FIGURE 4 Showing how, in this case, the sinusoidal shape of the second differential of the reflecting surface in (b) may be deduced from the relative positions of the cusps in the caustic focus (a).

differential, the distribution of stress normal to the plate can be obtained. On the other hand, by integrating twice, the deformation field itself can be obtained.

For the purposes of measuring dimensional changes associated with water uptake by coatings on the chip on board, we first have to map out the caustic focus and then invert it in order to obtain the surface profile.

There are two ways by which caustic foci can be inverted into surface profiles, namely, integration and iteration.[6] If the geometry of the caustic focus is amenable to standard curve fitting procedures then, by twice integrating the second differential obtained directly from measured co-ordinates of the caustic focus, we can generate the surface profile. Since it is more generally useful, however, we will now describe the iteration method for obtaining surface profiles from caustic foci.

In Figure 5, consider a small number of rays reflected by a surface. Ray R_i, after reflection from point P_i on the surface, subtends an angle α_i to the X-axis. Rays, $R_{i+1}, \ldots, R_n$, similarly subtend angles $\alpha_{i+1}, \ldots, \alpha_n$ respectively. Each point on the reflecting surface, corresponding to a single ray, has its own unique inclination to the X-axis. The relationship between the local slope, θ_{i-1}, of the reflecting surface and the angle subtended by individual rays can be derived as follows.

$$X_i = \frac{Z_{i-1} - ((-\tan\alpha_i \pm (\tan^2\alpha_i + 1)^{1/2}))X_{i-1} - C_i}{\tan^2\alpha_i + (\tan^2\alpha_i + 1)^{1/2}}$$

$$Z_i = Z_{i-1} - ((\tan\alpha_i \pm (\tan^2\alpha_i + 1)^{1/2})) \qquad (15)$$

$$\left(\frac{Z_{i-1} - ((\tan\alpha_i \pm (\tan^2\alpha_i + 1)^{1/2}))X_{i-1} - C_i}{\tan^2\alpha_i + (\tan^2\alpha_i + 1)^{1/2}} - X_{i-1}\right)$$

where $\tan\alpha_i$, X_{i-1}, Z_{i-1}, and C_i, can be obtained by $(i-1)^{th}$ iteration. For $i=0$, $X_i=0$, Z_i can be adjusted until the asymptotic curve of the surface profile closes to zero after the n^{th} iteration.

It is evident that very high accuracy, for inversion of the caustic focus into the reflecting surface that gives rise to it, can be achieved if $(X_i - X_{i-1})$ is very small. By way of illustration of the accuracy offered by this method, Figure 6 shows two surface profiles, one being the original that gives rise to the caustic, and the other being the experimentally-determined surface obtained by inverting the caustic focus.

To estimate the precision offered by this new method for measuring surface profiles, error analyses have been carried out by considering a small random error made in the co-ordinate measurements for a caustic focus. For example, consider a random error of ± 20 μm in the X-direction co-ordinate. Using the cubic spline method to smooth the experimental curve, and the iteration procedure, we derive the two surface profiles associated with the error ± 20 μm. The deviation, (Z′–Z), at a number of points has been calculated and is presented in Figure 7. These results indicate that a measurement error of ± 20 μm generates an error, in the Z-direction in the derived surface profile, of only 0.50 μm.

Now consider how small a deformation of the reflecting surface might be detectable by our method. Consider a specimen with a deformed surface described by

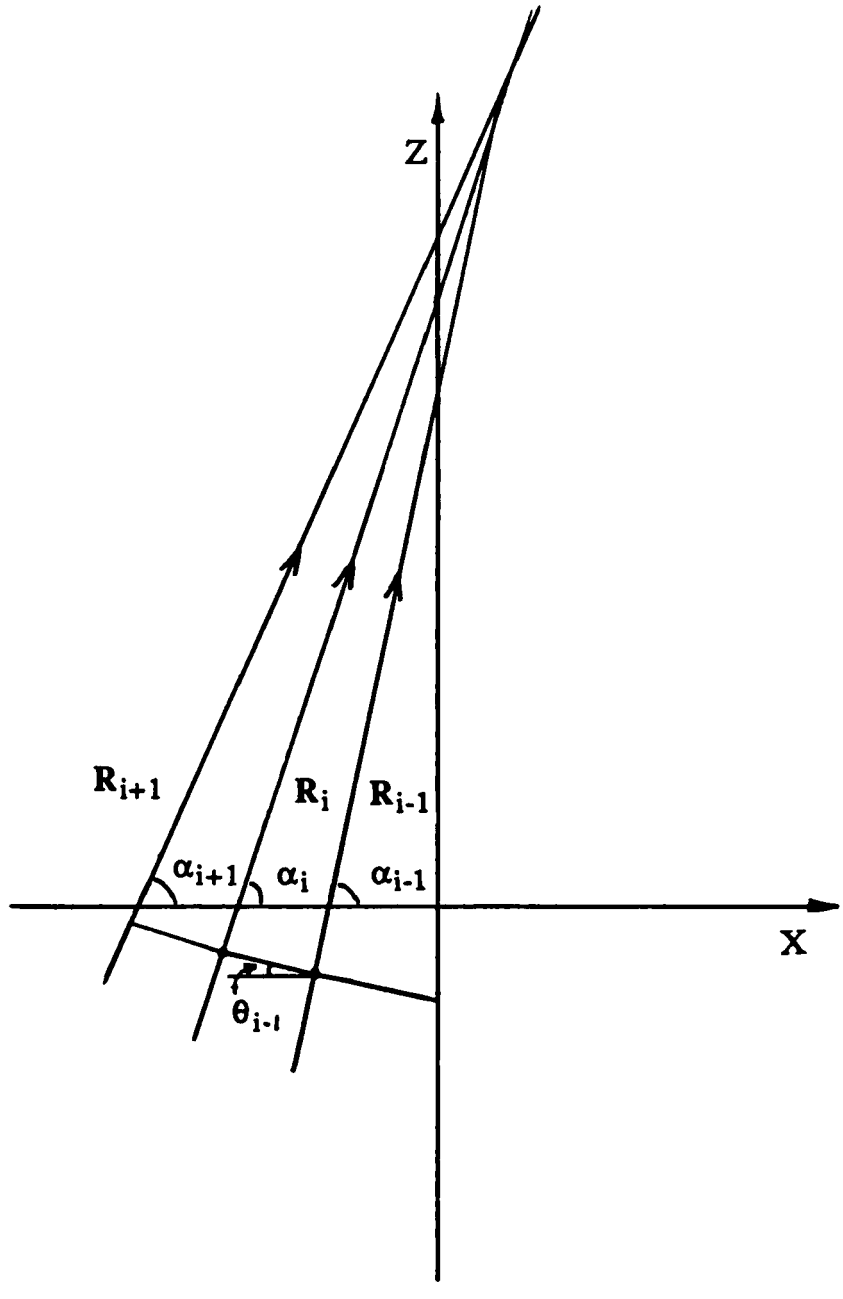

FIGURE 5 Generation of surface profile from a caustic focus by iteration.

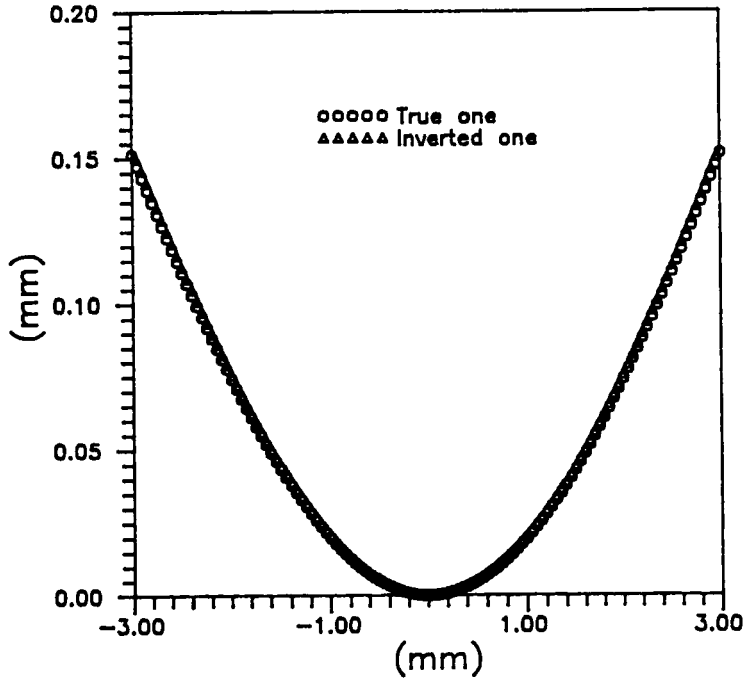

FIGURE 6 Comparison of the inverted surface profile obtained from caustic foci measurement and its true surface profile.

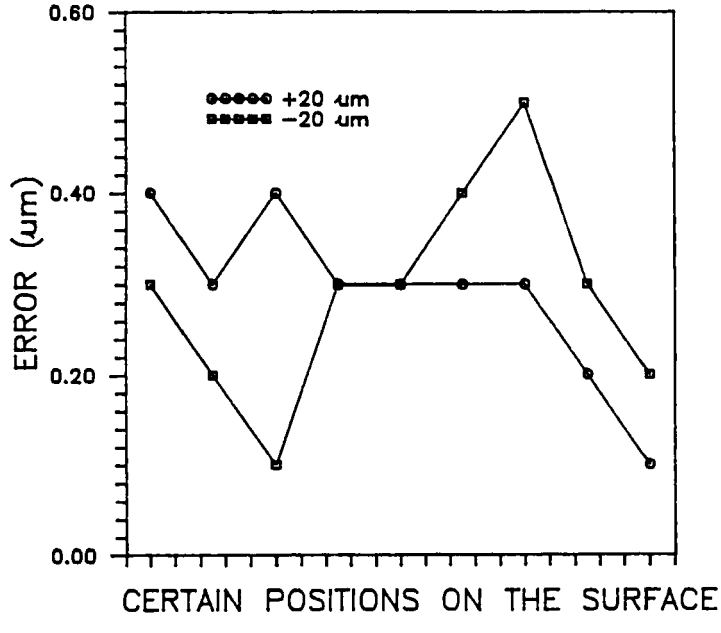

FIGURE 7 The deviation of experimentally determined surface profile at various sites, that is caused by the measurement error $\Delta x = \pm 20$ μm.

$Z = -H \exp(-x/w)$, and $w = 3$ mm. Figure 8 shows that for, say, 1 m from the specimen surface in a typical experiment, a displacement of 10 nm at the specimen surface can be detected if the corresponding displacement of caustic focus, 10 μm, can be recorded.

If it contains one, the cusp in a caustic focus provides a unique method for measurement of small deformations. Referring to Figure 9, the cusp is at infinity when the specimen surface is flat. When deformation of the specimen begins, the cusp moves rapidly towards the specimen surface.

APPLICATION TO THE MEASUREMENT OF DIMENSIONAL CHANGES

The technique can be used because of the smoothly curved edges of the coating, in all probability a geometry fortuitously dictated by the wettability of the substrate. It is reflection, by the curved edge to form a caustic focus, that we have successfully exploited in order to measure the surface distortion associated with small water uptake by the coating.

Figure 10 shows a computer simulation of a transparent coating illuminated by

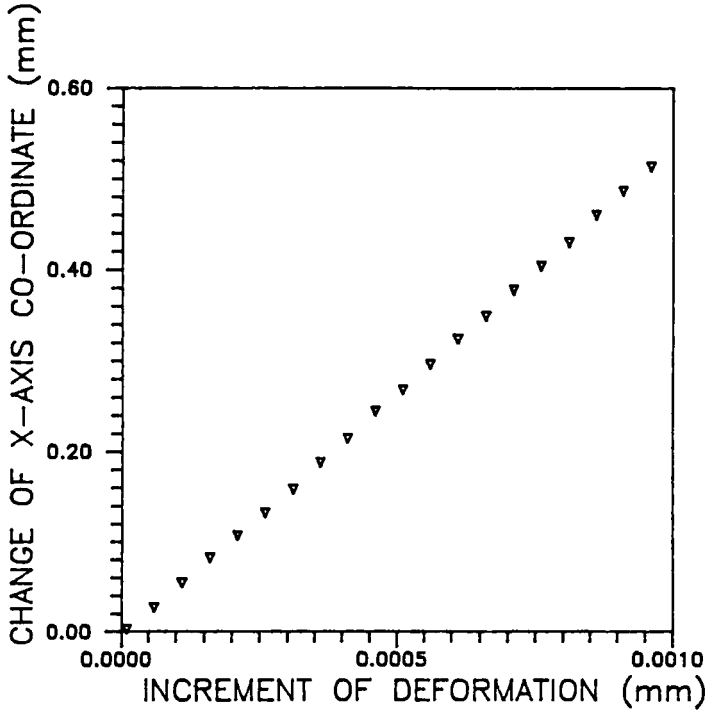

FIGURE 8 The change, with increments of reflecting surface deformation, of x-axis co-ordinate of the caustic focus.

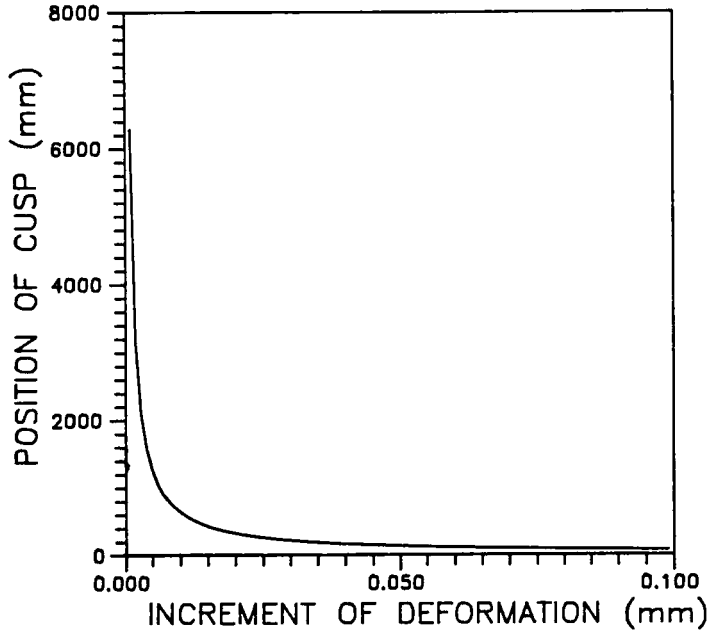

FIGURE 9 Displacement of a cusp in a caustic focus as a function of deformation of the reflecting surface.

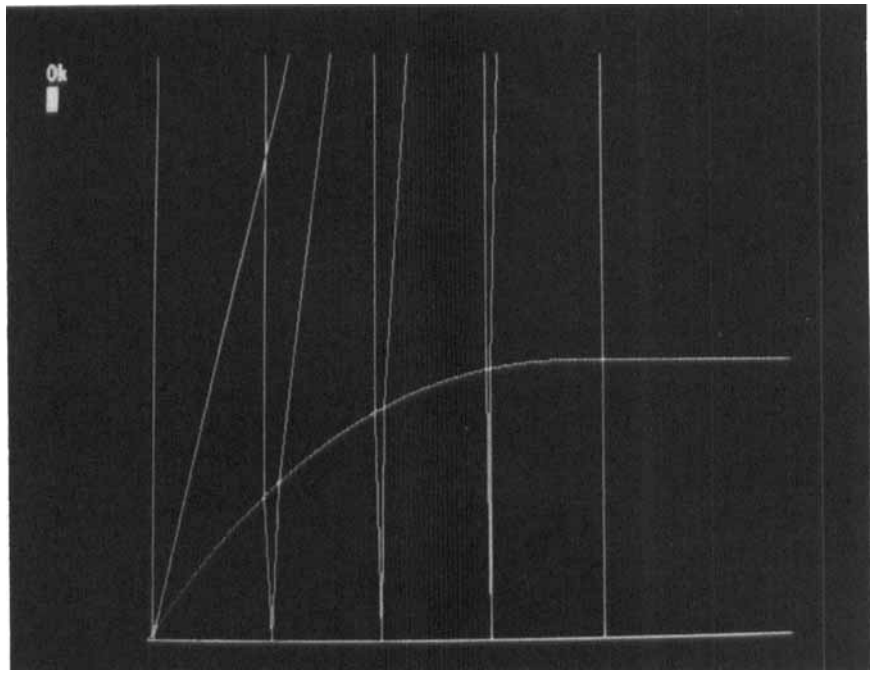

FIGURE 10 Computer simulation showing the propagation of rays through a transparent coating that has a smoothly curved edge.

parallel light refracted at the surface of the coating and reflected at the substrate (See Figure 11).

Consider the effects of all the interfaces between water, coating, an optical flat and air. Correspondence between the points of the coating and the focus plane S_f, shown in Figure 11, is given by

$$U - X = (Z_1 - S)\tan\alpha + Z_2\tan\beta + Z_3\tan\gamma \tag{16}$$

where S = the thickness of the coating,
$Z_1 - S$ = the depth of immersion water,
Z_2 = the thickness of the optical plate,
Z_3 = the distance from the optical flat to the caustic focus,
α, β, γ = the reflected and refracted angles at the interfaces.

Using exactly the same approach as before, the equation to the caustic focus can be obtained. The relationship is given by[6]

$$Z_3 = \left(-1 - (Z_1 - S)\frac{1}{\cos^2\gamma}\frac{d\gamma}{dx} + \frac{dS}{dx}\tan\gamma + Z_2R_1\frac{(M)^{1/2}\dfrac{d\gamma}{dx}\cos\gamma + \dfrac{R_1\sin^2\gamma\cos\gamma\dfrac{d\gamma}{dx}}{(M)^{1/2}}}{M}\right)/T \tag{17}$$

where

$$T = R_1R_2\frac{(N)^{1/2}\dfrac{d\gamma}{dx}\cos\gamma + \dfrac{R_1R_2\sin^2\gamma\cos\gamma\dfrac{d\gamma}{dx}}{(N)^{1/2}}}{N}$$

$$M = 1 - (R_1\sin\gamma)^2$$

$$N = 1 - (R_1R_2\sin\gamma)^2$$

$$R_1 = \frac{n_0}{n_1}$$

$$R_2 = \frac{n_1}{n_2}$$

$N_0 = 1.00$, $n_1 = 1.52$, and $n_2 = 1.30$ are the refractive indices for air, optical flat and water, respectively.

The computer-generated ray diagram and the corresponding caustic focus formed by the protective coating are shown in Figure 12. The computed changes of caustic focus associated with uniform swelling due to water absorption are shown in Figure 13. For a change in coating thickness from 40 μm, the original thickness, to 44 μm causes the caustic focus to be displaced vertically by 20 μm, an easily detected

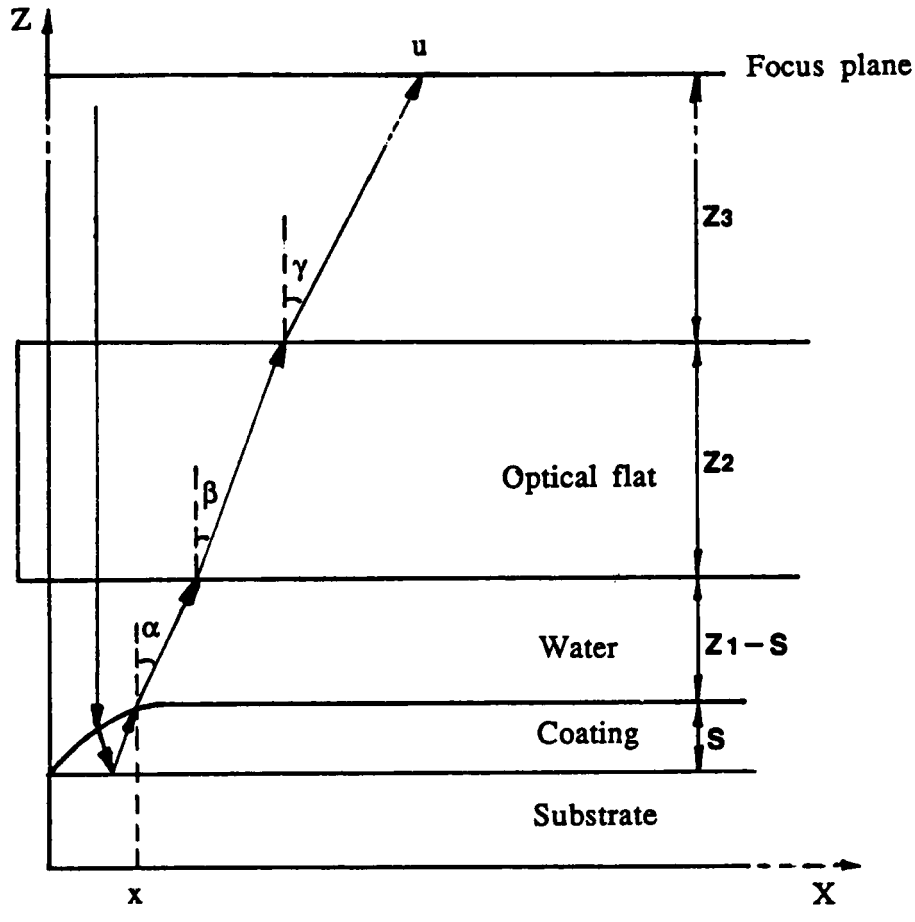

FIGURE 11 Propagation of a ray striking the specimen at normal incidence.

change. The accuracy of measurement is of the order discussed in the previous section.

Figure 14 shows the geometric relationship between the incident ray, the reflecting surface and the ray emerging from the coating surface. To invert the caustic focus into a a surface profile, an assumption has to be made. Referring to Figure 14, the relationship between the orientation of the emergence ray and surface profile can be derived[6] as follows

$$\alpha_1 = \frac{\pi}{2} - (\sin^{-1}(\sin(\tan^{-1}(S_{1x}) - \sin^{-1}(\frac{n_2}{n_3}\sin(\tan^{-1}(S_{1x})))$$

$$+ \tan^{-1}(S_{2x}))\frac{n_3}{n_2})) + \tan^{-1}(S_{2x}) \qquad (18)$$

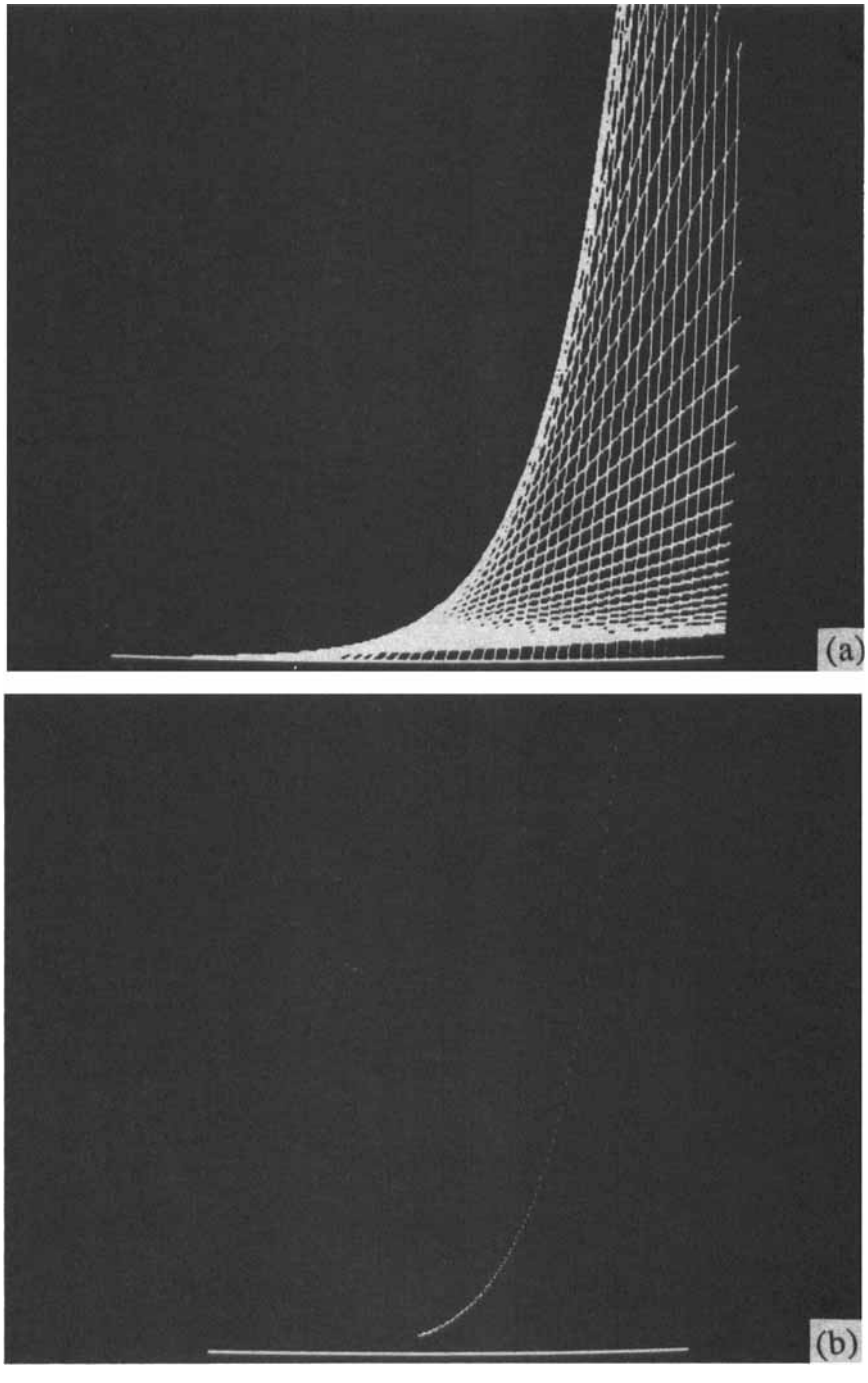

FIGURE 12 The computer generated ray diagram (a) and corresponding caustic focus (b) formed by the protective coating.

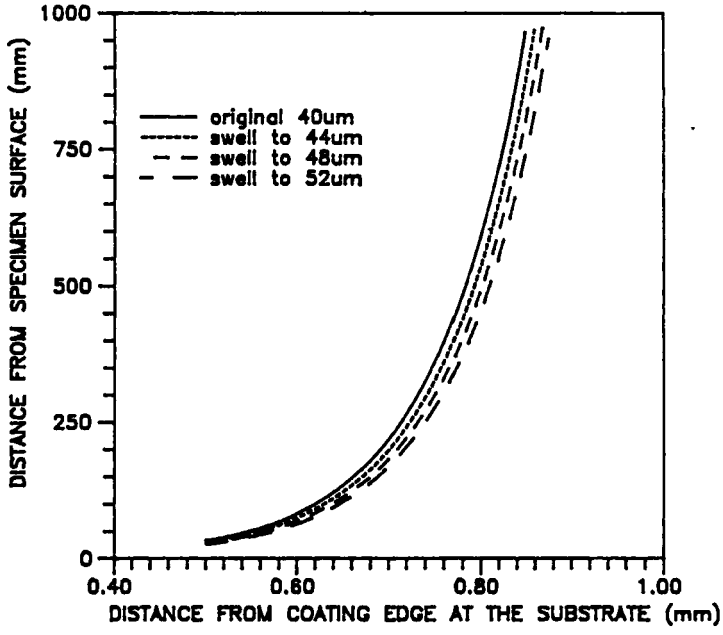

FIGURE 13 Change of caustic associated with uniform swelling of coating during water uptake.

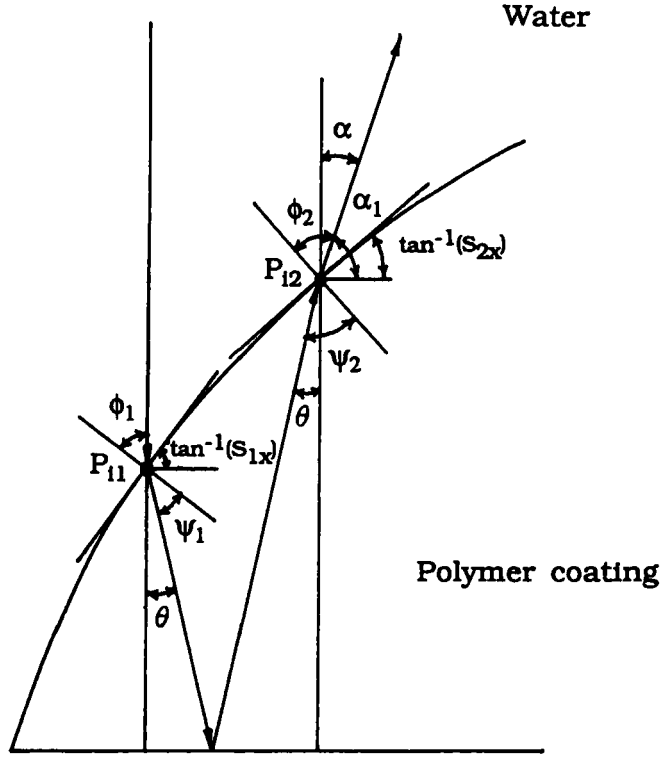

FIGURE 14 The geometry used to deduce Equation (18).

where S_{1x}, and S_{2x} are the slopes at the points P_{i1} and P_{i2}, and $n_3 = 1.55$ is the refractive index for polymer coating. Since the coating thickness is very small, about 30–40 μm, the points, P_{i1} and P_{i2}, defined by the incidence and emergence of ray i (refer to Figure 14), are sufficiently close together for their slopes to be regarded as approximately equal. With this approximation, the slope at P_{i2} can be calculated from the caustic focus.

As pointed out in the previous section, this method can be used to measure very small displacements, as small as 10 nm. Also, since the caustic focus is directly related to the second differential of displacement of the reflecting surface, our method offers significant advantages when the stress in the coating (given by the fourth differential of its displacement) is required.

RESULTS AND DISCUSSION

The caustic foci generated by the smoothly-curved edges of polymer coatings on the COB during water immersion have been recorded both periodically by photographing and continuously by video recording. The caustics were generated using the optical system sketched in Figure 15. The laser provides monochromatic light and the temperature of the environmental chamber, in which the specimen is immersed in distilled water, is automatically controlled.

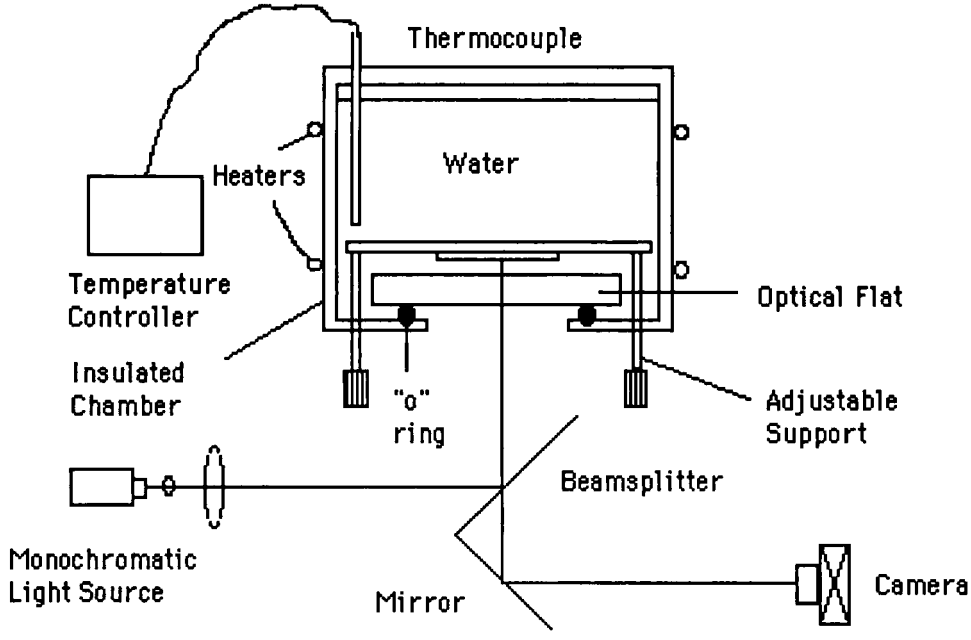

FIGURE 15 Optical system used to generate and simultaneously record interference fringe patterns and caustics from COB coatings.

TABLE I

Specimen	Prior treatment	Investigating technique	Investigating technique
#1	11 days in humidity chamber		Caustic Foci
#2	Control Sample	Moire Fringes	Caustic Foci
#3	11 days in salt spray chamber	Moire Fringes	Caustic Foci
#4	None		Caustic Foci
#5	None	Moire Fringes	

Five specimens, identified in Table I, have been investigated.

Most, if not all, organic coatings are permeable to moisture. Apart from swelling in order to accommodate the presence of water, the coating slowly permits access of water to, and probably corrosion of, the underlying substrate. Depending on the Pelling-Bedworth ratio, the products of corrosion are likely to bolster the swelling. In such cases, the overall swelling, and hence the measured change in caustic geometry, is attributable partly to the coating and partly to the substrate.

The volumetric swelling associated with substrate corrosion has been investigated using the multiple-beam interferometry technique,[6] as illustrated in Figure 15, but with a coated optical flat.

Figure 16 schematically shows multiple-beam interference generated in the space

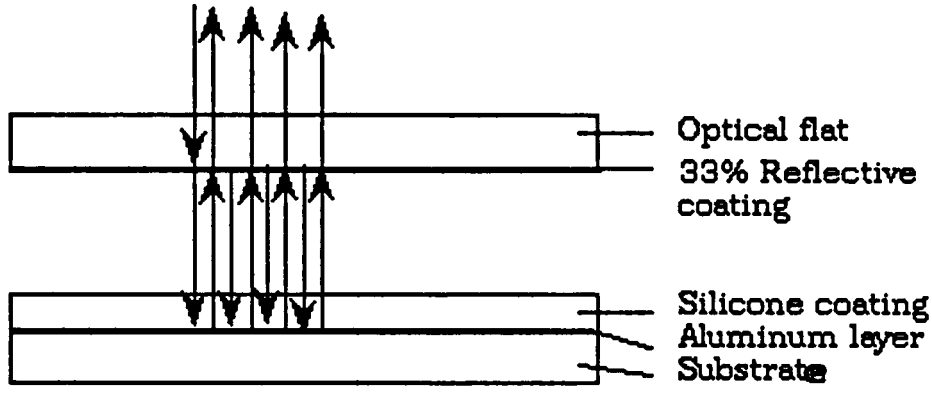

FIGURE 16 Multiple-beam interference generated in the space (water + transparent coating) between an optical flat and a highly reflective coated substrate.

between an optical flat and a highly reflective surface coated with transparent polymer. Each of a set of parallel reflected rays bears a fixed phase relationship to all the other rays. The phase differences arise from optical path length differences after the various reflections. The waves are coherent and, if collected and brought to a point focus by a lens, an interference pattern is obtained. Although the optical interference pattern itself can be used to study the topography of the reflecting surface, the following moire fringe method is more convenient in practice. When two nearly identical periodic patterns are superimposed one on the other, moire fringes are formed. The spatial distribution of moire fringes, which are contours of the specimen with contour level with respect to a reference flat differing by ½ λ from a dark or bright fringe to the next, faithfully follows normal displacement of the specimen surface.

Experimental results, for example, for specimen #2, obtained by using multiple beam interference to generate moire fringes, are shown in Figure 17. The average displacement in the direction normal to the specimen plane, obtained by dividing the swelling volume obtained by integrating the displacement by the area exposed to water, see Figure 18, suggests that the effects of post-curing treatments of specimens #2, #3 and #5, on the absorption of water by the substrate materials, are not significant.

Figure 19 shows schematically the formation of the caustic focus generated by the curved edges of the coating on the COB. Figure 20 is typical of the observed caustic focus so generated from sample #1. The geometry of the caustic focus can be obtained by measuring its size at different distances from the specimen using either conventional photography or a video camera. Figure 21 presents the data from the caustic focus for sample #4 after different water immersion times. The coating surface profiles obtained by inverting the caustic focus as outlined in the previous section, are presented in Figures 22–25. We note from the measurement results that the coatings on samples #1, #2, #3 and #4 appear to be of different as-received thickness. There are two possible explanations for this. Either the thickness is not well controlled by the coating process, or the reference point from which measurements are made is different for each sample. The absolute values for the increase in coating thickness attributable to water uptake, however, are reliable since these values are not changed significantly if the edge points of the surface profiles are extrapolated to a reasonable point in order to make the original coating thicknesses identical.

Since the samples have been treated under different conditions, see Table I, the coatings are expected to exhibit different responses to water immersion tests. These differences have been demonstrated by comparing the normal displacement well within the uniformly flat region of surface coating, as shown in Figure 26. Sample #3, which had been subjected to 11 days salt spray, has lowest swelling rate, *i.e.*, smallest slope in Figure 26, and lowest saturated value of water uptake. Sample #1, which had been exposed for 11 days in a humidity chamber, has lower swelling rate and lower saturated value of water uptake. Although samples #2 and #4 have almost identical swelling rates, the saturated water contents are different. This latter difference may be attributed to the effects of different post-curing treatments.

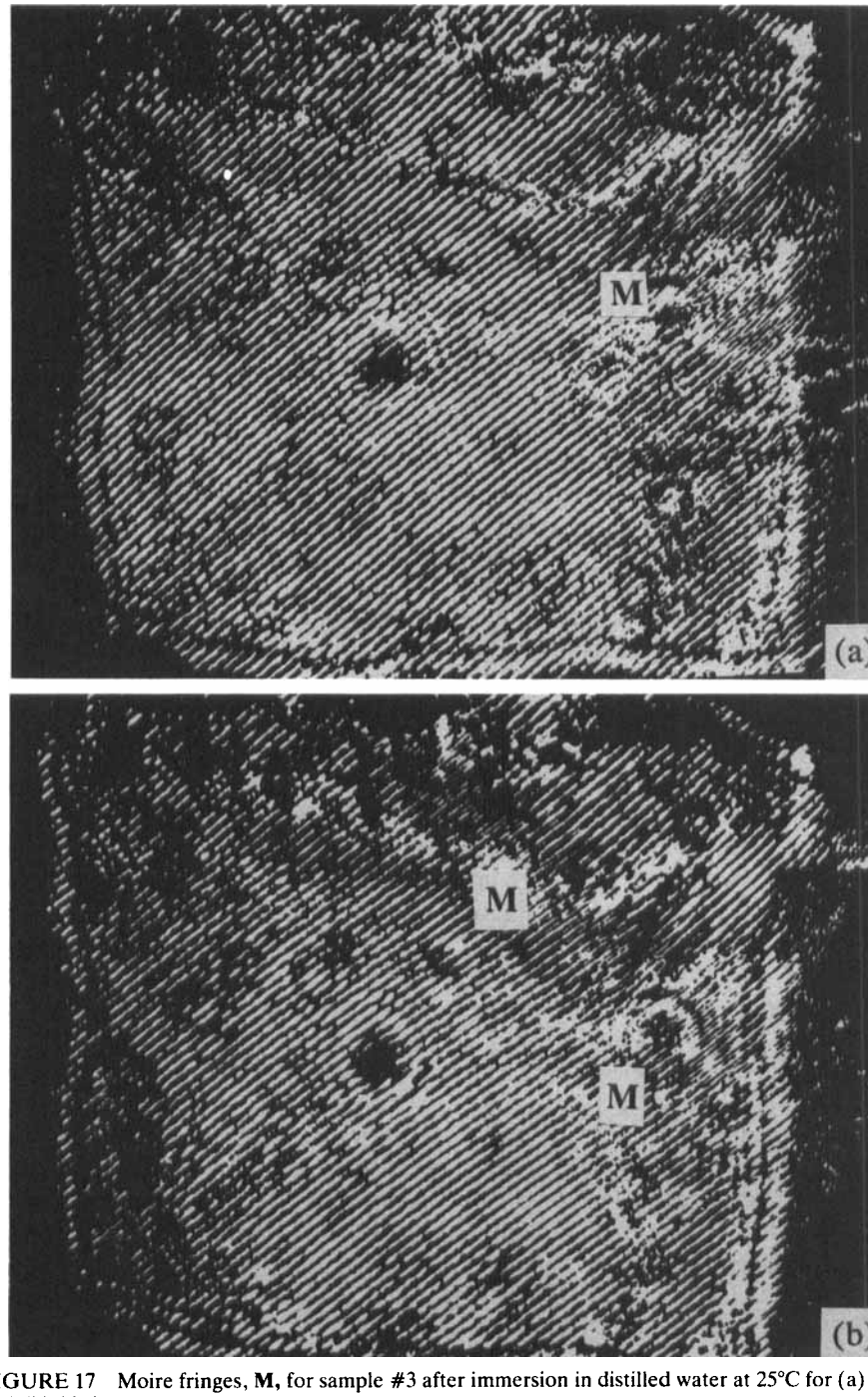

FIGURE 17 Moire fringes, **M,** for sample #3 after immersion in distilled water at 25°C for (a) 10 days and (b) 20 days.

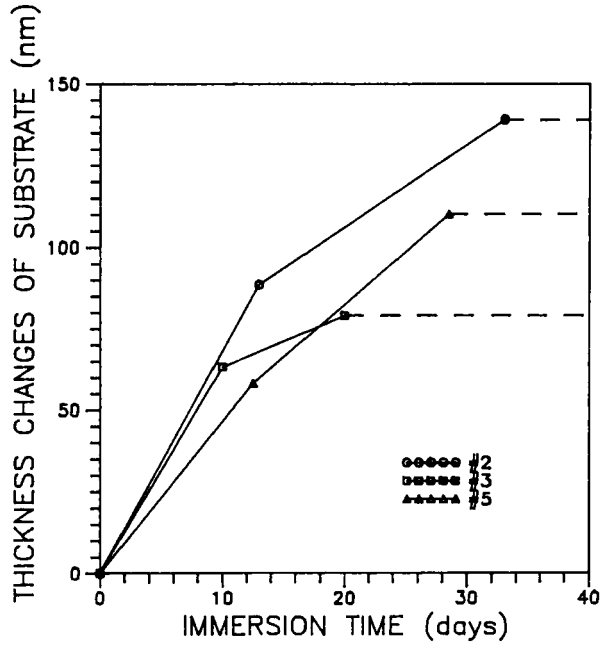

FIGURE 18 The thickness increase of the substrate during water immersion of samples #2, #3 and #5.

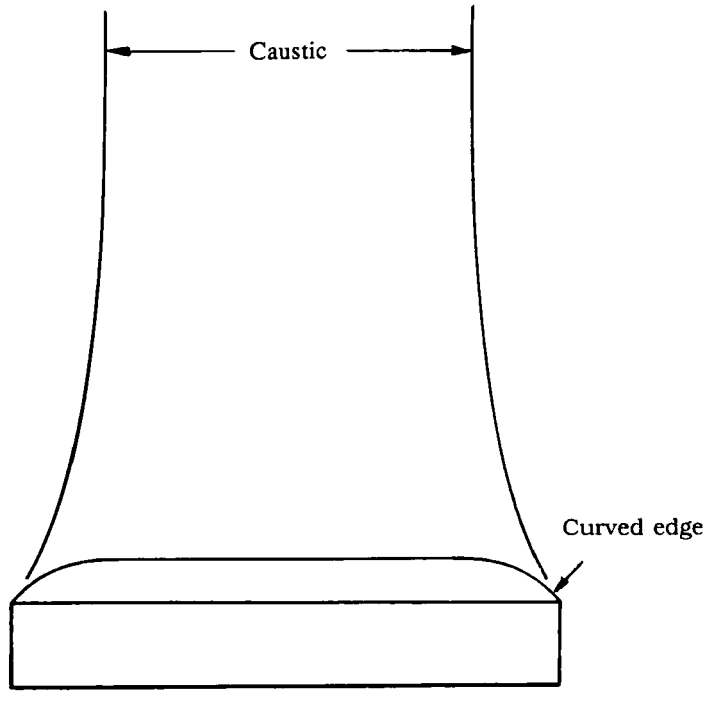

FIGURE 19 Schematic of the caustic focus generated by the curved edges of the COB.

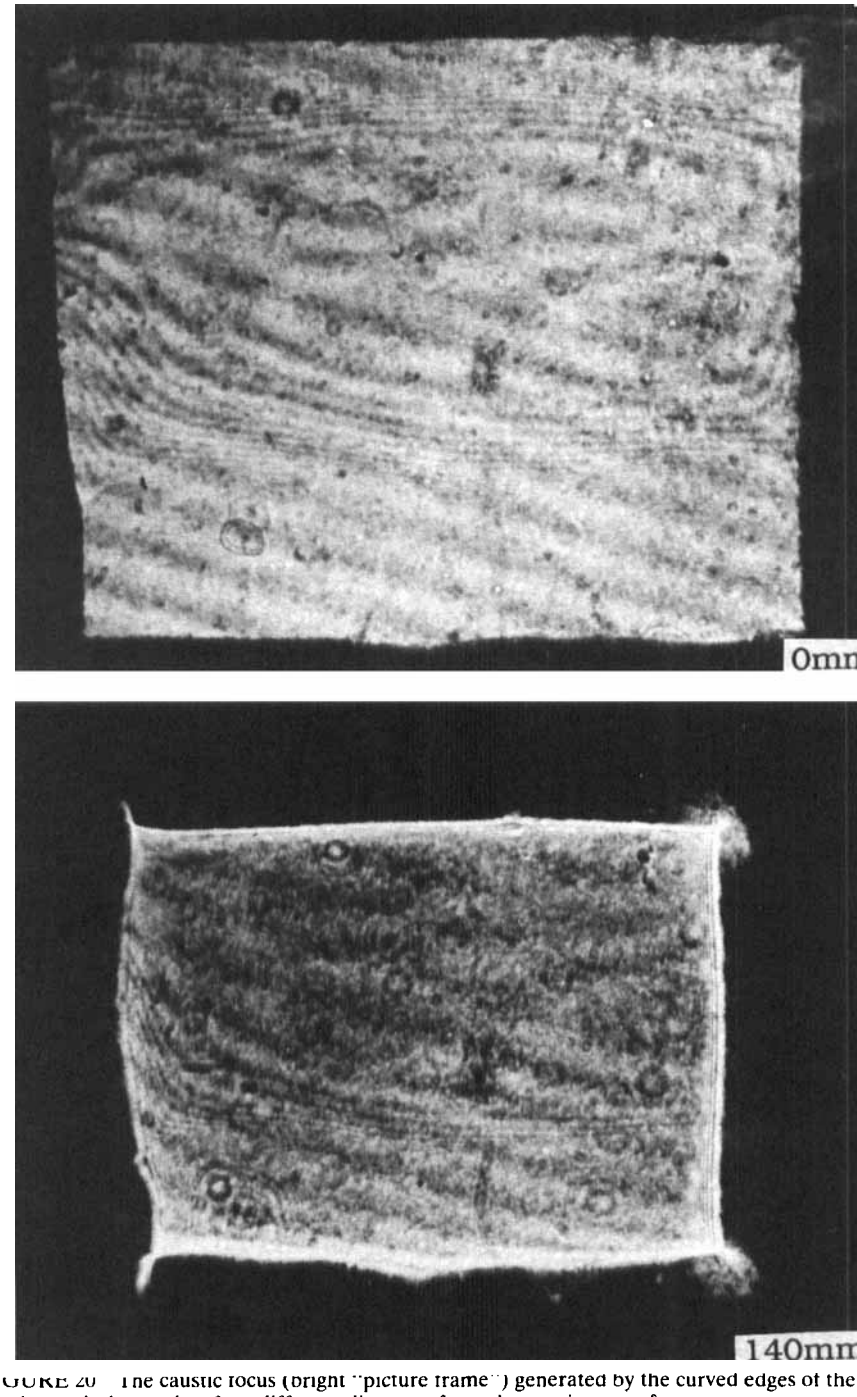

FIGURE 20 The caustic focus (bright "picture frame") generated by the curved edges of the polymer coating and observed at four different distances from the specimen surface.

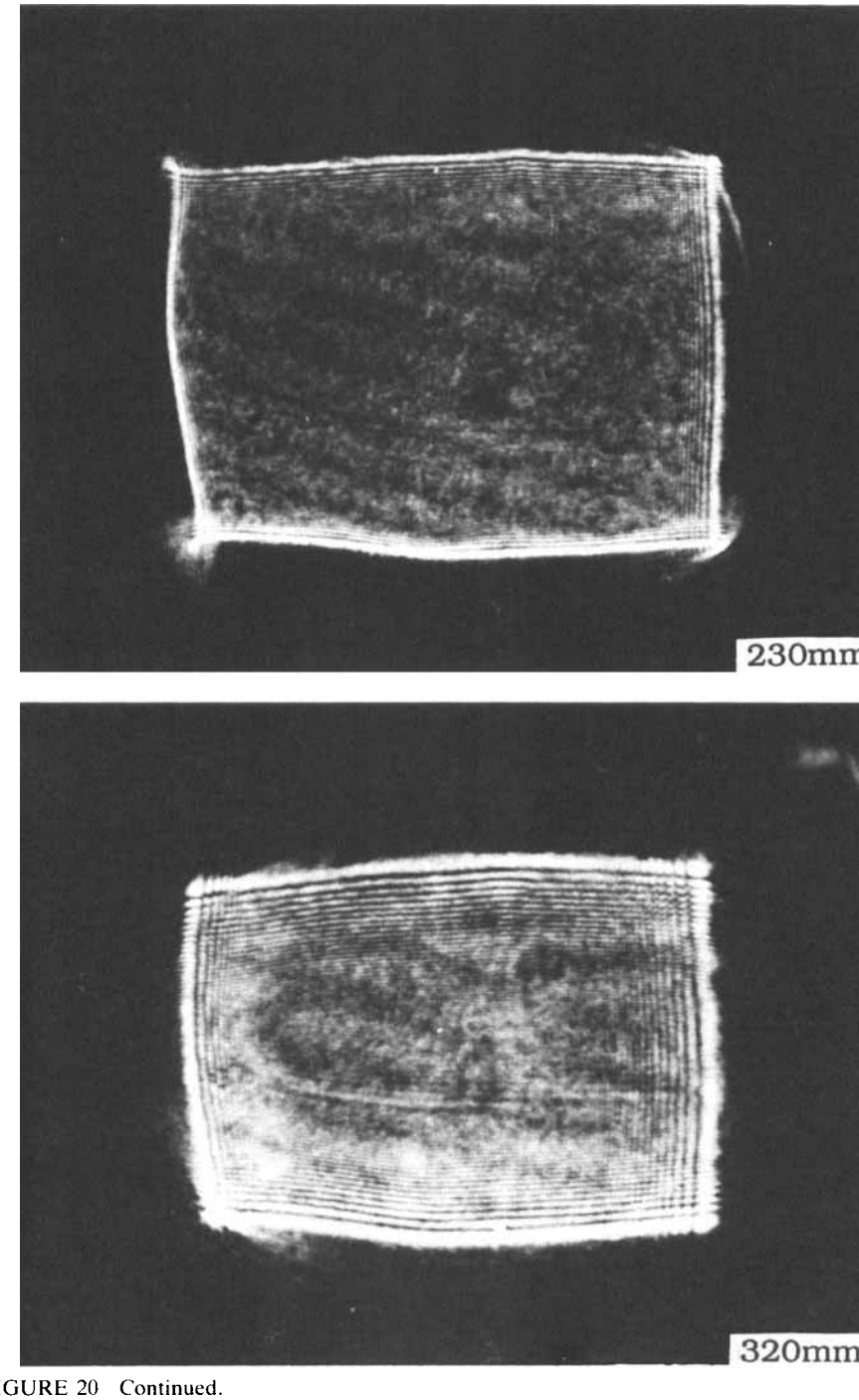

FIGURE 20 Continued.

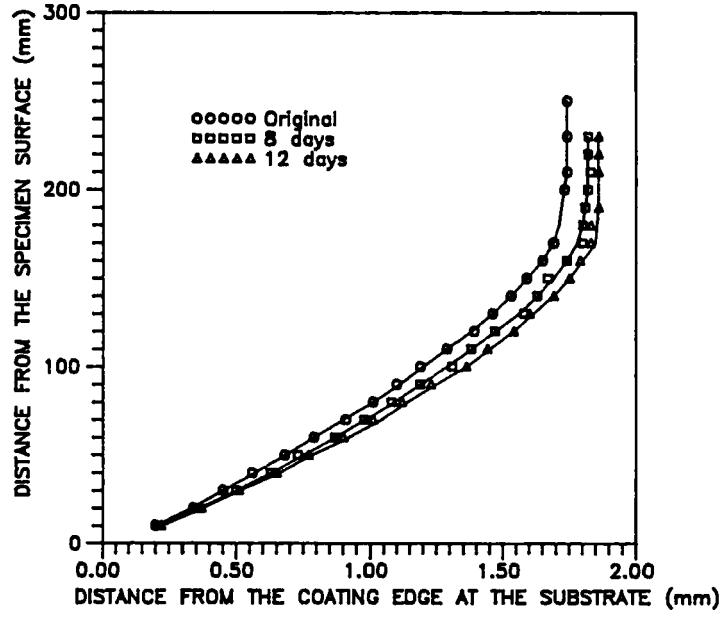

FIGURE 21 The measured caustic focus for sample #4 immersed in distilled water at 25°C.

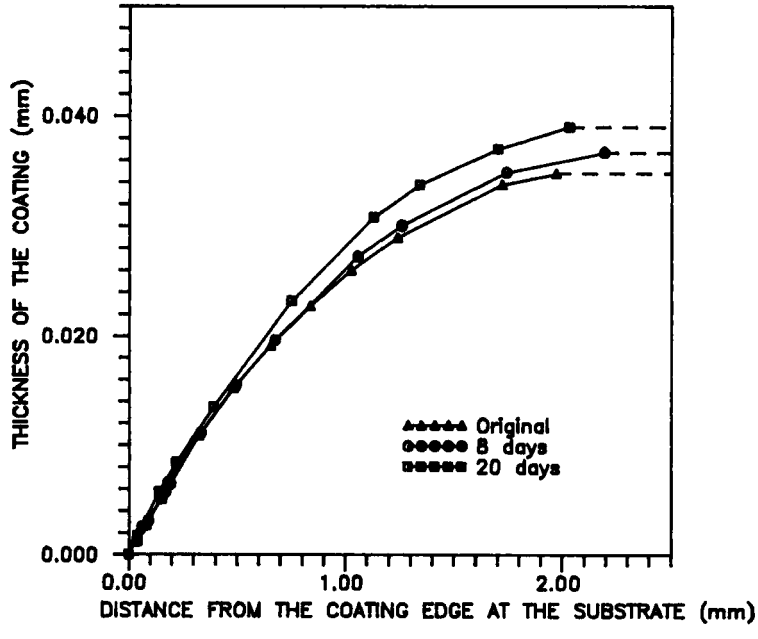

FIGURE 22 The surface profile of sample #1 obtained by inverting the measured caustic focus data.

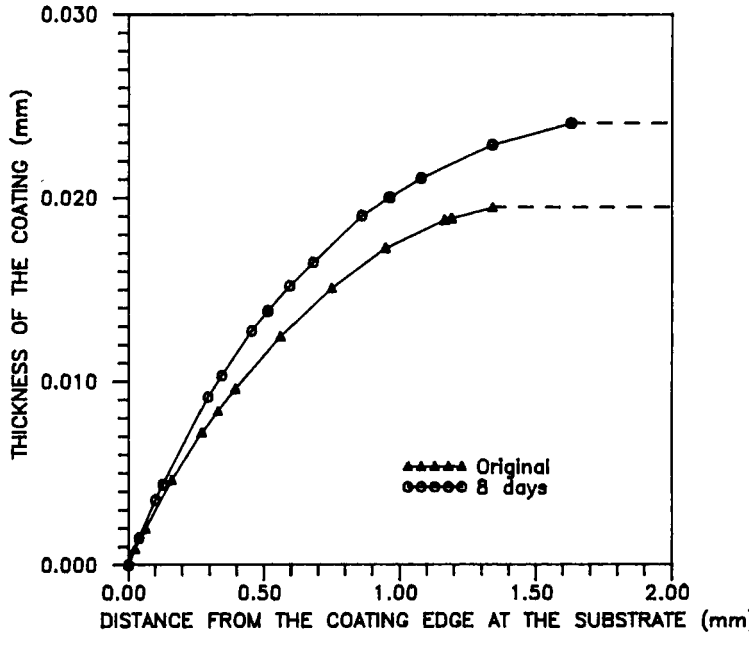

FIGURE 23 The surface profile of sample #2 obtained by inverting the measured caustic focus data.

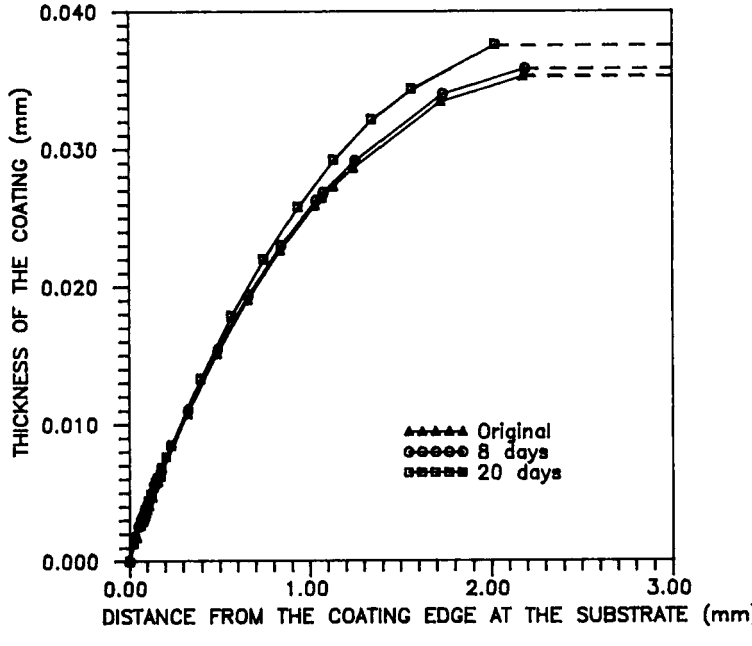

FIGURE 24 The surface profile of sample #3 obtained by inverting the measured caustic focus data.

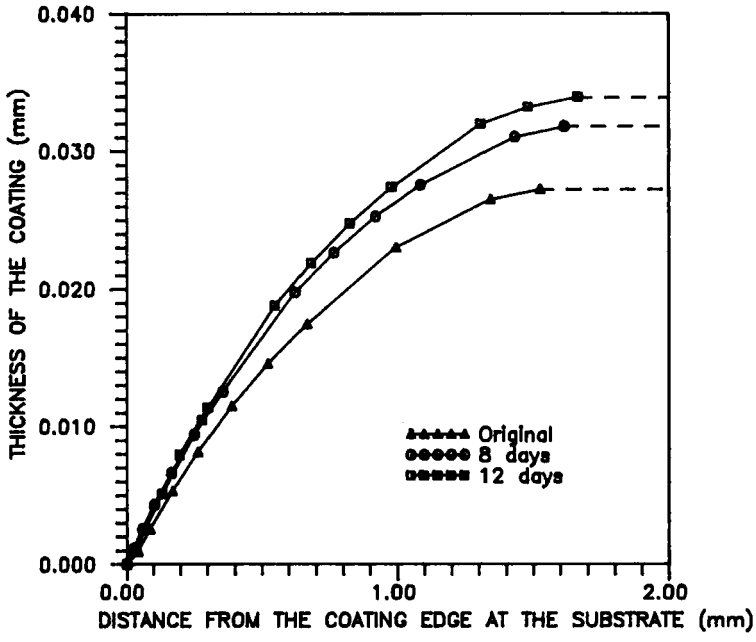

FIGURE 25 The surface profile of sample #4 obtained by inverting the measuring caustic focus data.

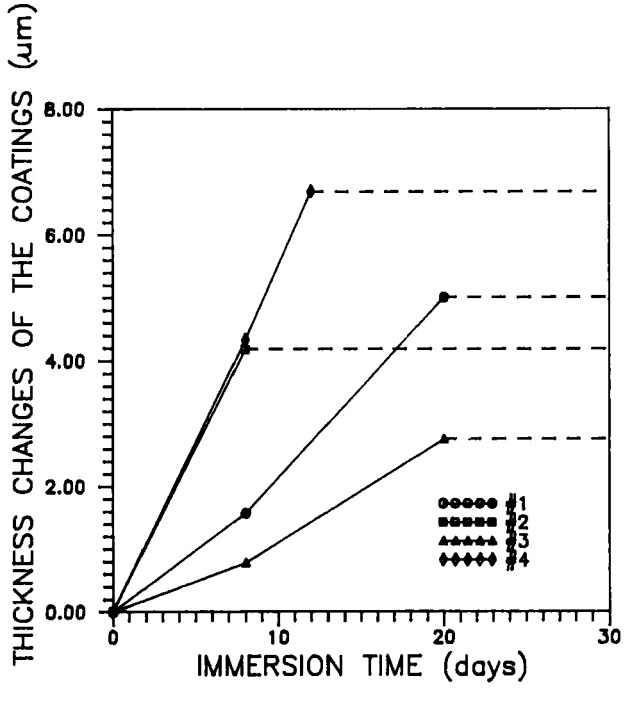

FIGURE 26 The coating thickness change due to water uptake for the different samples.

CONCLUSIONS

A new technique to measure small dimensional changes using optical caustic foci has been developed. The mathematical analysis of the technique suggests that the procedure, measuring the caustic size and then inverting to obtain the reflecting surface profile, is reliable. The accuracy claimed for this measurement is great and could be further improved if, instead of the caustic focus itself, its diffraction pattern were analyzed.[7,8]

The new technique has been successfully used to measure dimensional changes accompanying water uptake by polymer coatings on chip-on-board (COB) components. The optical interference technique described in previous reports,[9,10] cannot be used for this purpose owing to the transparency of the coating material.

An investigation of the consequences of water uptake at the substrate, using multiple-beam interference and moire fringe techniques, shows that the resultant volumetric swelling is very small, the average increase in the thickness being 70–140 nm. Our primary investigation, of water uptake by coating materials using optical caustic foci, shows that dimensional changes of the coating material during water uptake can be successfully monitored and measured. The results reveal effects of post-curing treatments on the dimensional change rates, and hence on the water uptake rates, and on the saturated value for water uptake. The results also reveal that a sample subjected to 11 days salt spray has the lowest swelling rate and the lowest value of saturated water uptake, and that a sample treated for 11 days in a humidity chamber has a lower swelling rate and a lower value of saturated water uptake. These results are consistent with those presented in another report.[10]

Acknowledgement

This work was supported by the Martin Marietta Corporation and was monitored by Dr. M. Ibrahim.

References

1. E. Hecht, *Optics* (Addison-Wesley Publishing Co., 1987), Chap. 6, pp. 220–240.
2. P. Manogg, Dissertation, University Freiburg, 1964.
3. P. S. Theocaris, *J. Appl. Mech.*, **37,** 409 (1970).
4. J. F. Kalthoff, J. Beinert and S. Winkler, *ASTM STP 627* (ASTM, Philadelphia, 1977), p. 167.
5. J. R. Brewster, M. S. Thesis, University of Tennessee, 1989.
6. Z. R. Xu, Ph. D. Dissertation, University of Tennessee, 1991.
7. L. D. Landau, E. M. Lifshitz and M. Hamermesh, *The Classical Theory of Fields* (Pergamon Press, 1962), pp. 165–172.
8. T. Pearcey, *Phil. Mag.*, **37,** 131 (1946).
9. K. H. G. Ashbee and D. A. Tossell, "High Performance Fiber Reinforced Materials," Report to Martin Marietta Laboratories, Contract No: UTK-87-002C, Dec. 31, 1988.
10. K. H. G. Ashbee and Z. R. Xu, "High Performance Fiber Reinforced Materials," Final Report to Martin Marietta Laboratories, Contract No: UTK-87-002C, Nov. 1, 1989.